

Match me if you can: Semantic Correspondence Learning with Unpaired Images

Jiwon Kim^{1†}, Byeongho Heo², Sangdoo Yun², Seungryong Kim³, Dongyoon Han²

¹LG AI Research, ²NAVER AI Lab, ³Korea University

Abstract

Recent approaches for semantic correspondence have focused on obtaining high-quality correspondences using a complicated network, refining the ambiguous or noisy matching points. Despite their performance improvements, they remain constrained by the limited training pairs due to costly point-level annotations. This paper proposes a simple yet effective method that performs training with unlabeled pairs to complement both limited image pairs and sparse point pairs, requiring neither extra labeled keypoints nor trainable modules. We fundamentally extend the data quantity and variety by augmenting new unannotated pairs not primitively provided as training pairs in benchmarks. Using a simple teacher-student framework, we offer reliable pseudo correspondences to the student network via machine supervision. Finally, the performance of our network is steadily improved by the proposed iterative training, putting back the student as a teacher to generate refined labels and train a new student repeatedly. Our models outperform the milestone baselines, including state-of-the-art methods on semantic correspondence benchmarks.

Introduction

Learning dense correspondences between image pairs is a fundamental problem that facilitates many computer vision tasks (Yang and Ramanan 2019; Kim et al. 2019; Lee et al. 2020; Li et al. 2020b; Min, Kang, and Cho 2021; Xie et al. 2021; Kokkinos and Kokkinos 2021). In contrast to classical dense correspondence tasks, where images are captured in geometrically constrained settings such as different views of the same scene (Hosni et al. 2012; Melekhov et al. 2019) or neighboring frames in a video (Ilg et al. 2017; Sun et al. 2018; Hui, Tang, and Loy 2018), the semantic correspondence task (Liu, Yuen, and Torralba 2010; Bristow, Valmadre, and Lucey 2015; Hur et al. 2015; Ham et al. 2017) finds pixel-wise visual correspondences between images containing the same object or semantic meaning. Due to these unconstrained settings, it should handle the additional challenges of large intra-class variations in appearance and background clutter. Recent deep learning-based matching models (Min et al. 2019a; Liu et al. 2020; Li et al. 2020a; Min and Cho 2021; Li et al. 2021; Zhao et al. 2021; Min et al. 2020; Cho et al. 2021; Cho, Hong, and Kim 2022), following data-driven approach, were generally trained in a supervised fashion based on datasets (Ham et al.

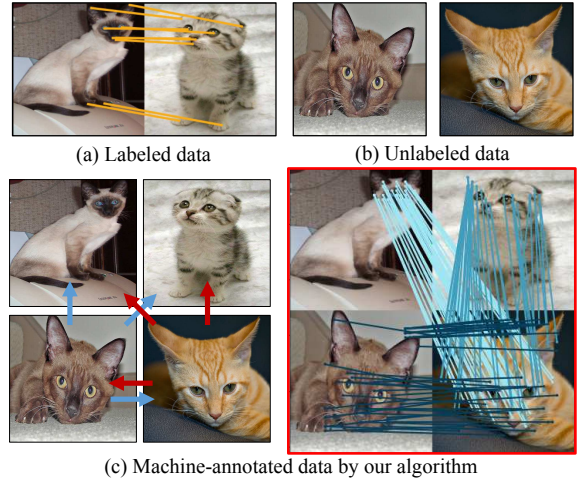


Figure 1: **How do we get more supervision?** We conjecture that dense correspondence learning usually suffers from data hunger. (a) Labeled data in the SPair-71k benchmark (Min et al. 2019b) consists of images and sparse manually-annotated keypoint annotation pairs. (b) Unlabeled images would become additional data sources for dense correspondence. (c) Newly expanded data by MatchMe from the unlabeled images can provide additional densified points for training. Blue and red arrows indicate newly acquired image pairs per each unlabeled data. Red box shows the machine-annotated labels that can be created when a new unlabeled image is added.

2017; Min et al. 2019b) providing limited training pairs with manually annotated keypoint matches as shown in Fig. 1(a). While the constraints imposed by pixel-level semantic correspondences are strict, the manual annotation by experts incurs significant time and expenses, limiting the amount of available training data.

To overcome the lack of labeled image pairs, various methods focused on unsupervised strategies (Rocco, Arandjelovic, and Sivic 2017; Jeon et al. 2020; Sarlin et al. 2020; Laskar and Kannala 2018; Truong et al. 2022; Kim et al. 2022; Huang et al. 2022) to increase the amount of correspondences supervision on unlabeled data in a self-supervised or weakly-supervised way. In particular, the weakly-supervised methods attempted to solve the label sparsity problem by using a cycle consistency (Laskar and Kannala 2018; Truong et al. 2022) or pseudo-labels (Kim et al. 2022; Huang et al. 2022) on real image pairs for unsupervised loss signal, but they only

[†] Work done while at NAVER AI Lab. Correspondence to Dongyoon Han: dongyoon.han@navercorp.com.

rely on image pairs provided by the dataset. The capability of heavy matching networks hinges on data quantity at first, but the training data remains significantly smaller than other computer vision tasks (*e.g.*, 1.2M images in ImageNet-1K (Russakovsky et al. 2015)). Therefore, we argue that previous approaches (Laskar and Kannala 2018; Kim et al. 2022; Truong et al. 2022; Huang et al. 2022), attempting to densify points for training, may not be an underlying solution for the data-hungry problem.

In this paper, we present a fundamental approach that focuses on overcoming the insufficiency of both image pairs and point pairs, different from previous methods (Laskar and Kannala 2018; Kim et al. 2022; Truong et al. 2022; Huang et al. 2022). Our key idea is that a large corpus of unlabeled image pairs, having rich semantic information, has not been fully used since they remain unannotated. For example, an unlabeled image newly supplied, shown in Fig. 1(b), can be utilized to generate new pairs with originally labeled or other unlabeled images; the newly created pairs can be used for providing densified labels for training as shown in Fig. 1(c). Based on the observation, we propose a simple yet effective framework dubbed MatchMe machine-generating point-level supervision on unlabeled image pairs without the inflow of extra manually labeled data.

To acquire pseudo correspondences for training pairs without human annotations, we adopt the concept of a teacher-student training (Tervainen and Valpola 2017; Xie et al. 2020b; Pham et al. 2021; Li et al. 2022), using a pair of networks. First, we train a matching network with given labeled data and assign it to a teacher after training. Next, we use the teacher to generate machine-annotated correspondences on unannotated image pairs. We conjecture first that a machine annotator has some degree of labeling reliability based on the literature (Xie et al. 2020b; Yun et al. 2021). Finally, we train a student model using the pseudo correspondences as supervision on unannotated image pairs. To further improve the quality of generating pseudo correspondences, we repeat this process multiple times, with the student model taking the role of the teacher for the upcoming iteration.

We evaluate our method by applying it to recent matching architectures (Cho et al. 2021; Cho, Hong, and Kim 2022). Experimental results prove that our method is effective and achieves state-of-the-art performance on every benchmark, including PF-PASCAL (Ham et al. 2017), PF-WILLOW (Ham et al. 2017), and SPair-71k (Min et al. 2019b). MatchMe achieves state-of-the-art performance on all semantic correspondence benchmarks, showing accuracy gain of 2.0% and 2.4% on PF-WILLOW and SPair-71k (PCK@ $\alpha = 0.1$).

Related Work

Semantic correspondence learning. Recent methods for semantic correspondence (Min et al. 2019a; Liu et al. 2020; Li et al. 2020a; Min and Cho 2021; Li et al. 2021; Zhao et al. 2021; Min et al. 2020; Cho et al. 2021) inevitably train complicated matching networks to maximize performance in a supervised manner with limited qualified dataset (Ham et al. 2017; Min et al. 2019b), which leads to high computational demands and poor generalization capability across datasets.

Some unsupervised strategies (Laskar and Kannala 2018;

Truong et al. 2022; Kim et al. 2022; Huang et al. 2022) extend their unsupervised loss to the supervised regime and significantly improve the performance of the previous supervised approaches. This shows that the performance of the existing supervised model was not fully learned due to a lack of data. Specifically, the methods (Laskar and Kannala 2018; Truong et al. 2022) use a cycle consistency for unsupervised loss signal, and the others (Kim et al. 2022; Huang et al. 2022) utilize pseudo-labels, generated by the model’s prediction between real images, combined with confidence measures to guarantee the quality of pseudo-labels. Unlike previous methods (Laskar and Kannala 2018; Truong et al. 2022; Kim et al. 2022; Huang et al. 2022), we introduce a fundamental approach to address the lack of both image and point pairs by utilizing massive unlabeled data.

Self-training methods. Self-training (Tervainen and Valpola 2017; Xie et al. 2020b; Pham et al. 2021; Li et al. 2022), which is often used in semi-supervised learning, has a teacher-student structure, unlikely to pseudo-labeling (Lee et al. 2013; Shi et al. 2018) and consistency regularization methods (Rasmus et al. 2015). The separate teacher model, trained on a small set of labeled data, generates pseudo-labels on a large set of unlabeled data to guide the student model, and then the student is jointly trained on a combination of labeled and pseudo-labeled images. Recent studies have applied the teacher-student framework for pixel-level semi-supervised learning, specifically for the semantic correspondence task (Li et al. 2021; Huang et al. 2022). They employ a teacher model to generate additional pseudo-labels using knowledge from keypoint periphery (Huang et al. 2022) or hypotheses (Li et al. 2021) across labeled image pairs. On the other hand, our method labels overlooked unlabeled data using a machine annotator, continually repeating the process by assigning the learned student back to the teacher.

Background

Task Definition

The semantic correspondence task aims to predict the matching probability P between a semantically similar image pair. Given a training image pair \mathcal{S} with source image $I_s \in \mathbb{R}^{H_s \times W_s}$ and target image $I_t \in \mathbb{R}^{H_t \times W_t}$, a matching function f with the network parameters θ predicts $P_{s,t} = f(I_s, I_t; \theta) \in \mathbb{R}^{H_s W_s \times H_t W_t}$ by considering the feature similarities across all the points in I_s and I_t . It minimizes the following problem with the image pairs \mathcal{S} and supervision $\hat{P}_{s,t} \in \mathbb{R}^{H_s W_s \times H_t W_t}$ between two images (I_s, I_t) :

$$\mathcal{L}_{\mathcal{S}} = \frac{1}{|\mathcal{S}|} \sum_{(I_s, I_t) \in \mathcal{S}} \sum_{i=1}^{H_t W_t} \hat{M}_{s,t}(i) \mathcal{D}(P_{s,t}(\cdot, i), \hat{P}_{s,t}(\cdot, i)), \quad (1)$$

where (\cdot, i) indicates the i -th column of a matrix and $\mathcal{D}(\cdot, \cdot)$ is a distance function. $\hat{M}_{s,t} \in \mathbb{B}^{H_t W_t}$ denotes a binary mask vector, in which $\hat{M}_{s,t}(i)$ corresponds to the existence of $\hat{P}_{s,t}(\cdot, i)$; we have

$$\hat{M}_{s,t}(i) = \begin{cases} 1, & \text{if } \|\hat{P}_{s,t}(\cdot, i)\|_{\infty} > 0, \\ 0, & \text{otherwise.} \end{cases} \quad (2)$$

In a supervised learning framework, (I_s, I_t) is tied together, so minimization in Eq.(1) gives a matching function f under the fixed and limited image pairs \mathcal{S} .

Motivation

Previous methods aimed to design a novel matching network to gain a high-quality correlation map based on high-dimensional convolutions or Transformers. However, they leverage complicated learning frameworks with large models and distinct data augmentations due to relying on limited annotated keypoint pairs. Sophisticated learning frameworks (Kim et al. 2022; Huang et al. 2022; Truong et al. 2022) or heavy models (Rocco et al. 2020; Min and Cho 2021; Cho et al. 2021; Cho, Hong, and Kim 2022) with a strong matching function f , can fit a model to insufficient data space more; involving data augmentation methods (Kim et al. 2022) diversify the images I_s and I_t . However, they do not take into account the cardinality of the image pairs $|\mathcal{S}|$; still, the recent unsupervised methods that try to densify keypoint pairs (Kim et al. 2022; Huang et al. 2022) in each image pair do not consider the additional image pairs.

We claim that using the fixed annotated pairs in training inherently restricts prediction performance; this is more likely because the existing annotated pairs are sparse (Ham et al. 2017; Min et al. 2019b). We further conjecture that simple machine supervision (Xie et al. 2020b; Yun et al. 2021) could sufficiently give newly annotated point pairs, where the process does not need the aid of complex confidence measures or heavy network architectures.

Rather solving Eq.(1), we reformulate the problem as:

$$\min_{\theta, S'} \frac{1}{|\mathcal{S}'|} \sum_{(I_s, I_t) \in \mathcal{S}'} \sum_{i=1}^{H_t W_t} \hat{M}_{s,t}(i) \mathcal{D}(P_{s,t}(\cdot, i), \hat{P}_{s,t}(\cdot, i)), \quad (3)$$

where the objective has a newly added variable \mathcal{S}' and corresponding supervision. However, optimization of this problem seems like an NP-hard problem. Therefore, we relax the problem by managing the image pair variable to be expanded, having a lower bound of Eq.(1) by simply untying the link between source and target image pairs:

$$\min_{\theta} \frac{1}{|\mathcal{S}'|} \sum_{(I_s, I_t) \in \mathcal{S}'} \sum_{i=1}^{H_t W_t} \hat{M}_{s,t}(i) \mathcal{D}(P_{s,t}(\cdot, i), \hat{P}_{s,t}(\cdot, i)), \quad (4)$$

where $\mathcal{S}' \supseteq \mathcal{S}$. Minimizing Eq.(4) clearly reaches the trained weight with a lower value than minimizing Eq.(1). A larger cardinality has a lower objective value. Our concern now moves on to how to acquire additional pair sets in \mathcal{S}' over the original paired images \mathcal{S} .

Method

This section proposes a simple yet effective method for dense correspondence. Our method utilizes a machine annotator for an expanded set that includes unseen pairs across the entire images for training a target network.

Labeling Unlabeled Data

We present how to expand additional point pairs in unlabeled data employing a machine annotator by a teacher model

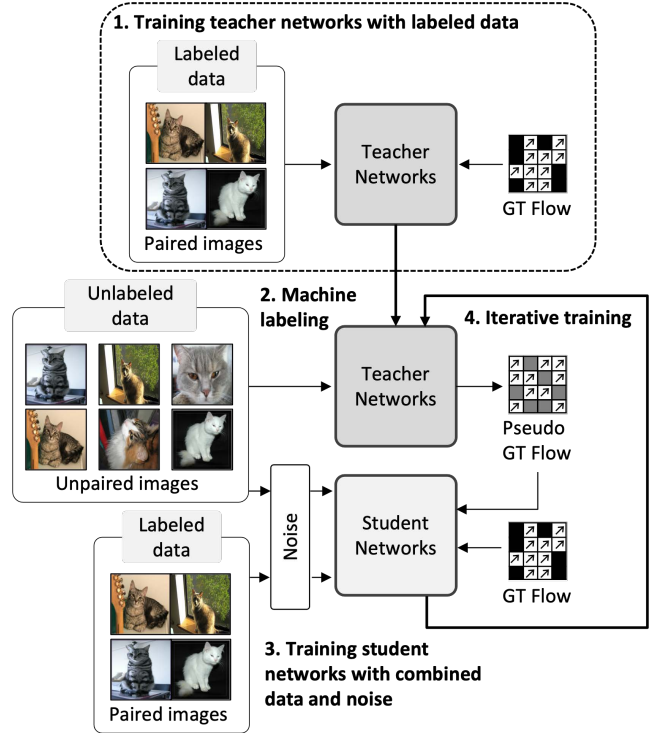


Figure 2: **Schematic illustration of the proposed method.** Our proposed method performs iterative training with the unlabeled images labeled by a machine annotator repeatedly.

learned from labeled data. Suppose we have a superset that contains massive images for training with or without labels having C object classes; there are n_c image samples in each class c . Ideally, $n_c(n_c - 1)$ pairs for each class could be utilized for supervised training (with labels). Namely, the possible image pairs for class c is

$$\mathcal{U}_c = \{(I_s, I_t) \mid s \in c, t \in c, s \neq t\}, \quad (5)$$

and the set of entire pairs in a training set is $\mathcal{U} = \bigcup_{c=1}^C \mathcal{U}_c$. The prior methods (Huang et al. 2019; Min et al. 2019a; Li et al. 2020a; Min et al. 2020; Zhao et al. 2021; Min and Cho 2021; Cho et al. 2021; Cho, Hong, and Kim 2022; Lee et al. 2021) only trained in the semantic correspondence benchmarks (Ham et al. 2017; Min et al. 2019b) share the general training protocol using the image pairs having given annotated keypoint pairs, which are a subset of \mathcal{U} . This is clearly because the amount of keypoint-level supervision does not cover not only the entire image pairs in the superset but also all the pixel pairs. A set of labeled data \mathcal{S}_c for supervised training consists of image pairs for each class label c , which can be defined as a subset of \mathcal{U}_c :

$$\mathcal{S}_c = \{(I_s, I_t) \in \mathcal{U}_c \mid \|\hat{M}_{s,t}\|_\infty > 0\}, \quad (6)$$

and the total set of image pairs is $\mathcal{S} = \{\mathcal{S}_c\}_{c=1}^C$. As aforementioned, this bottlenecks the model's maximal performance due to insufficient training image pairs to establish full dense correspondences under large intra-class variations (Min et al. 2020; Lee et al. 2021; Cho, Hong, and Kim 2022).

Therefore, expanding the training pairs towards the entire pairs \mathcal{U} is an obvious option. There can be an approach of picking which image pairs to use in training, but we simply involve the image set closer to the entire image pairs \mathcal{U} to show such a simple choice work. We further conjecture that this is more likely to cover different appearances and difficulty levels between image pairs, enabling the learned model to have improved generalizability.

To generate correspondence supervisions for newly expanded training pairs having no human annotations, we utilize a teacher network f_T as a machine annotator. f_T , which is pre-trained on labeled training pairs, generates pseudo correspondences $\bar{P}_{s,t} = f_T(I_s, I_t; \theta_T) \in \mathbb{R}^{H_s W_s \times H_t W_t}$ on newly involved training pairs where a large fraction of pairs do not belong to the existing training pairs. The student f is then trained to learn pseudo-labeled correspondences with

$$\mathcal{L}_{\mathcal{U}} = \sum_{(I_s, I_t) \in \mathcal{U}} \sum_{i=1}^{H_t W_t} \bar{M}_{s,t}(i) \mathcal{D}(P_{s,t}(\cdot, i), \bar{P}_{s,t}(\cdot, i)), \quad (7)$$

where $P_{s,t} = f(I_s, I_t; \theta)$ is the predicted correspondence from the model. We use $\bar{M}_{s,t}$ as the binary mask for gating the correspondence based on a confidence-based strategy, widely used in (Xie et al. 2020a; Sohn et al. 2020; Rizve et al. 2021; Xu et al. 2021; Zhang et al. 2021). By using a matching confidence $\bar{C}_{s,t}(\cdot, i)$, which defined from pair-wise scores between all locations in I_s and i in I_t with soft-argmax operation, it is thus formulated as

$$\bar{M}_{s,t}(i) = \begin{cases} 1, & \text{if } \|\bar{C}_{s,t}(\cdot, i)\|_\infty > \tau, \\ 0, & \text{otherwise,} \end{cases} \quad (8)$$

where τ is the score threshold. The high-confidence pseudo correspondences encourage the model to be trained without erroneous supervision from ambiguous or textureless areas. In this work, different from the previous methods (Huang et al. 2019; Min et al. 2019a; Li et al. 2020a; Min et al. 2020; Zhao et al. 2021; Min and Cho 2021; Cho et al. 2021; Cho, Hong, and Kim 2022; Lee et al. 2021), trained on sparse keypoint pairs per limited labeled image pairs, we can significantly increase the number of image pairs available for training by including unlabeled data and also use a large corpus of keypoint pairs, densely filling most object parts by using the teacher model as the machine annotator without the expense of manual annotation made by a human expert.

Our training objective is $\mathcal{L} = \mathcal{L}_{\mathcal{U}} + \lambda \mathcal{L}_{\mathcal{S}}$ combining the loss function in Eq.(1) and Eq.(7) to leverage both the existing labeled pairs and the ones annotated by machine annotator. The weighting parameter λ adjusts the learning dynamics between the losses; we use $\lambda=1$ for simplicity.

Iterative Labeling and Training

We further propose an iterative training method inspired by the methods (Xie et al. 2020b; Tan and Le 2021) to improve the quality of the pseudo correspondences. Each iteration repeats the training process using the trained model in the previous iteration as a new teacher. We define l -th training iteration as (f_T^l, f^l) , consisting a pair of teacher-student network. The first generation of teacher model f_T^0 is trained on labeled training pairs \mathcal{S} , starting from scratch without a

teacher. The subsequent generations of teacher models use the model trained in the preceding generations, *i.e.*, $f_T^l = f^{l-1}$.

During training, we augment the input images of the student model to diversify them further and let the model learn with more challenging ones. We use photometric augmentation \mathcal{N}_p (Cho et al. 2021; Cho, Hong, and Kim 2022; Kim et al. 2022) and geometric augmentation \mathcal{N}_g (Rocco, Arandjelovic, and Sivic 2017; Kim et al. 2022; Truong et al. 2022), to the source and target image of the student network. As a result, the student is trained on more challenging image pairs than those in teacher training, which enhances the model’s generalization ability, resulting in a superior student surpassing the teacher. It can be defined as $P_{s,t} = f(\mathcal{N}_p(I_s), \mathcal{N}_p(\mathcal{N}_g(I_t)))$. The teacher’s labels $\bar{P}_{s,t}$ are warped to align spatial position changes by applying the same geometric transformation as the student.

Experiments

Experimental Setups

Benchmarks. Experiments are conducted on three standard benchmarks for semantic correspondence learning: PF-PASCAL (Ham et al. 2017), PF-WILLOW (Ham et al. 2017), and SPair-71k (Min et al. 2019b) consisting of image pairs with human-annotated keypoints from 20, 4, and 18 categories, respectively. As in previous works (Han et al. 2017), we split the PF-PASCAL dataset (Ham et al. 2017) into about 700, 300, and 300 images for training, validation, and testing, respectively. For the SPair-71k dataset (Min et al. 2019b), we use 53,340 for training, 5,384 for validation, and 12,234 for testing. To verify generalization capacity, the PF-WILLOW dataset (Ham et al. 2017) is used for testing only.

Evaluation metric. Following prior works (Min et al. 2019a), the percentage of correct keypoint (PCK@ α_k) is used for the evaluation metric by setting α_k , a tolerance margin, having a value $\in \{0, 1\}$. PCK can be computed as the ratio of correctly estimated keypoint pairs to the total number of keypoint pairs using the Euclidean distance between them within the pixel margin $\alpha_k \cdot \max(H_k, W_k)$. By setting $k \in \{\text{img, bbox}\}$, H_k and W_k are the width and height of either image or the object’s bounding box.

Implementation details. We integrate our method into two state-of-the-art backbones, CATs (Cho et al. 2021) and CATs++ (Cho, Hong, and Kim 2022) for comprehensive evaluations. We use the equivalent network architecture as the baselines (Cho et al. 2021; Cho, Hong, and Kim 2022) for both teacher and student models. For the teacher, we use the best-performing model’s weight trained in a supervised setting on labeled data for the initial teacher to generate labels for the student. For the teacher model, only weak photometric augmentations, such as color-jitter and gray-scale, are used with a given probability of 0.2 to prevent early over-fitting. In order to train the student model to surpass the teacher, we conjecture that stronger data augmentations should be required. Following the literature (Cho et al. 2021; Cho, Hong, and Kim 2022), a combination of strong photometric augmentation at a frequency of 0.4 is used along with geometric augmentation (Rocco, Arandjelovic, and Sivic 2017; Lee et al. 2019; Truong, Danelljan, and Timofte 2020). The confidence

Methods	All	Aero	Bike	Bird	Boat	Bottle	Bus	Car	Cat	Chair	Cow	Dog	Horse	MBike	Person	Plant	Sheep	Train	TV
HPF	28.2	25.2	18.9	52.1	15.7	38.0	22.8	19.1	52.9	17.9	33.0	32.8	20.6	24.4	27.9	21.1	15.9	31.5	35.6
SCOT	35.6	34.9	20.7	63.8	21.1	43.5	27.3	21.3	63.1	20.0	42.9	42.5	31.1	29.8	35.0	27.7	24.4	48.4	40.8
DHPF	37.3	38.4	23.8	68.3	18.9	42.6	27.9	20.1	61.6	22.0	46.9	46.1	33.5	27.6	40.1	27.6	28.1	49.5	46.5
PMD	37.4	38.5	23.7	60.3	18.1	42.7	39.3	27.6	60.6	14.0	54.0	41.8	34.6	27.0	25.2	22.1	29.9	70.1	42.8
MMNet	40.9	43.5	27.0	62.4	27.3	40.1	50.1	37.5	60.0	21.0	56.3	50.3	41.3	30.9	19.2	30.1	33.2	64.2	43.6
CHM	46.3	49.6	29.3	68.7	29.7	45.3	48.4	39.5	64.9	20.3	60.5	56.1	46.0	33.8	44.3	38.9	31.4	72.2	55.5
PMNC	50.4	54.1	35.9	74.9	36.5	42.1	48.8	40.0	72.6	21.1	67.6	58.1	50.5	40.1	54.1	43.3	35.7	74.5	59.9
CATs	49.9	52.0	34.7	72.2	34.3	49.9	57.5	43.6	66.5	24.4	63.2	56.5	52.0	42.6	41.7	43.0	33.6	72.6	58.0
CATs++	59.8	<u>60.6</u>	<u>46.9</u>	<u>82.5</u>	<u>41.6</u>	56.7	<u>65.1</u>	<u>50.4</u>	<u>72.8</u>	<u>29.2</u>	<u>75.9</u>	<u>65.3</u>	<u>62.6</u>	<u>50.9</u>	<u>56.1</u>	<u>54.6</u>	48.0	<u>80.8</u>	<u>75.0</u>
SemiMatch	50.7	53.6	37.0	74.6	32.3	47.5	57.7	42.4	67.4	23.7	64.2	57.3	51.7	43.8	40.4	45.3	33.1	74.1	65.9
SCORRSAN	55.3	57.1	40.3	78.3	38.1	51.8	57.8	47.1	67.9	25.2	71.3	63.9	49.3	45.3	49.8	48.8	40.3	77.7	69.7
MatchMe-CATs	53.0	52.8	40.2	73.9	32.6	51.9	62.8	49.3	70.0	26.8	68.0	56.0	57.1	47.3	42.6	42.3	38.0	76.2	67.1
MatchMe-CATs++	62.0	63.4	51.1	83.2	44.8	<u>53.1</u>	66.9	53.4	74.8	30.4	76.8	66.6	68.1	55.2	60.7	59.1	48.1	84.9	75.9

Table 1: **Comparison with state-of-the-art methods on SPair-71k.** Per-class and overall PCK ($\alpha_{bbox} = 0.1$) results are shown in the table. Numbers in bold indicate the best performance, and underlined ones are the second best. The averaged PCK of each MatchMe significantly improves the baselines by a large margin; ours outperforms the state-of-the-art methods, including both the supervised regime such as CATs (Cho et al. 2021), CATs++ (Cho, Hong, and Kim 2022) and the semi-supervised regime such as SemiMatch (Kim et al. 2022), SCORRSAN (Huang et al. 2022) in all but one class.

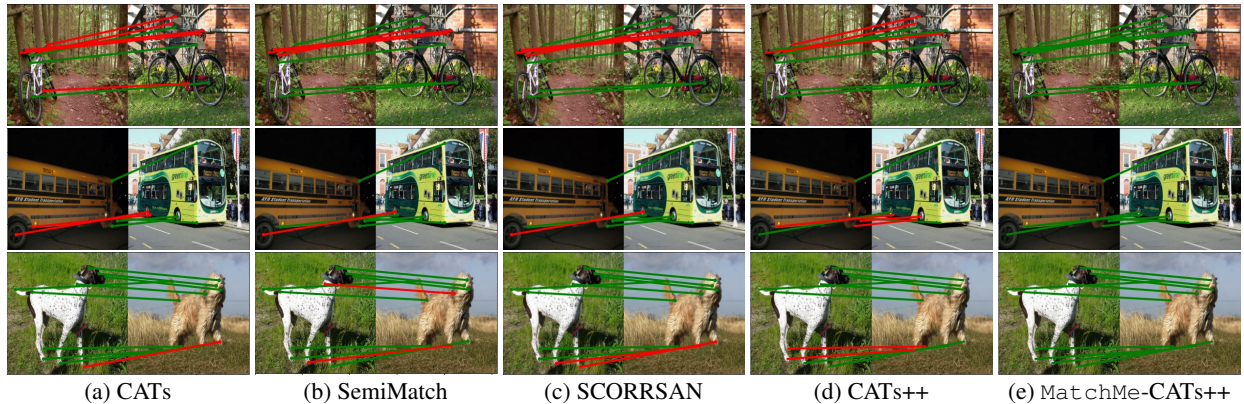


Figure 3: **Qualitative results on SPair-71k in comparison with SOTA methods:** The point-to-point matches are drawn by linking key point pairs with line segments. Green and red lines denote correct and incorrect predictions with respect to the ground-truth pairs, respectively. We observe that ours outperforms the counterparts significantly across all the sample image pairs.

threshold τ for pseudo correspondences is commonly set as 0.7 for all image pairs in training datasets. We employ the best pre-trained student as the teacher of the next generation and perform iterative training.

Comparison on Benchmarks

We evaluate our proposed model in comparison with the SOTA methods. The competing methods (Min et al. 2019a, 2020; Zhao et al. 2021; Min and Cho 2021; Cho et al. 2021; Cho, Hong, and Kim 2022) are trained based on the supervised protocol with keypoint annotations. We also compare with similar methods (Kim et al. 2022; Huang et al. 2022), using both generated labels and GT labels.

On SPair-71k. Tab. 1 shows the PCKs ($\alpha_{bbox}=0.1$) on all 18 object classes, including overall mean PCK. Our overall averaged PCK=**62.0%** significantly outperforms the current state-of-the-art methods. We achieve +2.2% and +3.1% of PCK improvements over the baselines (Cho et al. 2021; Cho, Hong, and Kim 2022), respectively. It demonstrates that the matching networks, especially with correlation enhancement architecture, have been under-trained with sparse and limited keypoint supervision. Outstanding PCKs on every class in-

dicate improved generalizability, which facilitates handling large intra-class variation and deformation between instances within the same object class.

Additionally, as shown in Fig. 3, we visualize the sampled example pairs with the predicted matches for MatchMe-CATs++ and the competing methods showing the best performance in both the supervised regime, such as CATs (Cho et al. 2021), CATs++ (Cho, Hong, and Kim 2022) and the regime similar to ours, such as SemiMatch (Kim et al. 2022), SCORRSAN (Huang et al. 2022), using both supervision from generated labels and GT keypoint labels. This demonstrates that our method estimates correspondences between image pairs more accurately than others, even under a large discrepancy in viewpoint and scale.

On PF-PASCAL and PF-WILLOW. Tab. 2 summarizes our results on the PF-PASCAL and PF-WILLOW datasets compared with the other competing methods trained on PF-PASCAL from each initialized model (*i.e.*, usually pre-trained on ImageNet (Russakovsky et al. 2015)). We also fine-tune our model, pre-trained on SPair-71k with the unlabeled data from PASCAL VOC 2012, on the PF-PASCAL dataset to evaluate the generalization capability of our model

Methods	PF-PASCAL			PF-WILLOW		
	α^{img}			α^{bbox}		
	0.05	0.1	0.15	0.05	0.1	0.15
HPF	60.1	84.8	92.7	45.9	74.4	85.6
DHPF	75.7	90.7	95.0	49.5	77.6	89.1
MMNet	77.6	89.1	94.3	-	-	-
CHM	80.1	91.6	-	52.7	79.4	-
CATs	75.4	92.6	96.4	50.3	79.2	90.3
CATs++	84.9	<u>93.8</u>	96.8	56.7	81.2	-
PMNC	82.4	90.6	-	-	-	-
SemiMatch	80.1	93.5	96.6	54.0	82.1	92.1
SCORRSAN	81.4	92.9	96.1	<u>54.1</u>	80.0	89.8
MatchMe-CATs	76.2	92.9	96.5	<u>54.1</u>	83.9	94.2
MatchMe-CATs++	84.9	94.3	<u>96.7</u>	59.6	<u>83.6</u>	92.9

Table 2: **Comparison with state-of-the-art methods on PF-PASCAL and PF-WILLOW.** Numbers in bold denote the best, and underlined ones are the second best. MatchMe-CATs++ outperforms the competing methods again, like in Spair-71k.

	Methods	PCK
(a)	CATs++	59.8
(b)	(a) + CNNGeoU	60.1 (+0.3)
(c)	(a) + PWarpC	60.5 (+0.7)
(d)	(a) + SCORRSAN	61.0 (+1.2)
(e)	(a) + MatchMe	62.0 (+2.2)

Table 3: **PCK comparison among training methods.** For a fair comparison, we use the fixed baseline CATs++ (Cho, Hong, and Kim 2022) for all semi-supervised training methods. All methods work upon the baseline, but ours performs the best.

on different datasets. MatchMe-CATs++ records the new state-of-the-art PCK value 94.3 that beats the previous state-of-the-art value of 93.8, which is almost saturated, on PF-PASCAL.

On PF-WILLOW, MatchMe outperform the baseline counterparts by 3.8% / 4.7% / 3.9% ($\alpha = 0.05/0.1/0.15$) for CATs (Cho et al. 2021) and by 2.9% / 2.4% ($\alpha = 0.05/0.1$) for CATs++ (Cho, Hong, and Kim 2022), respectively. Note that our method not only achieves higher PCK than the competing methods on PF-PASCAL but outperforms them by a more significant margin on PF-WILLOW. This signifies the generalization capability of our method and discloses that ours learns a general representation, which can be applied to various datasets, different from the baselines usually overfitted on a specific dataset.

Controlled experiments for learning methods. We conduct controlled comparisons between our method and existing semi-supervised methods (Laskar and Kannala 2018; Truong et al. 2021; Huang et al. 2022). All the methods are trained with the fixed baseline CATs++ (Cho et al. 2021) for a fair comparison to evaluate the methods’ uniqueness in improving each method’s performance without any potential influence from the model difference. We use Spair-71k (Min et al. 2019b), which contains fixed, sparsely-annotated pairs, for a comprehensive comparison. We strive to report the best results for each method via parameter searches.

Tab. 3 first shows MatchMe outperforms all the competitors. Specifically, (a) and (b), using a cycle consistency, and (c), using generated pseudo-labels as sources of unsupervised

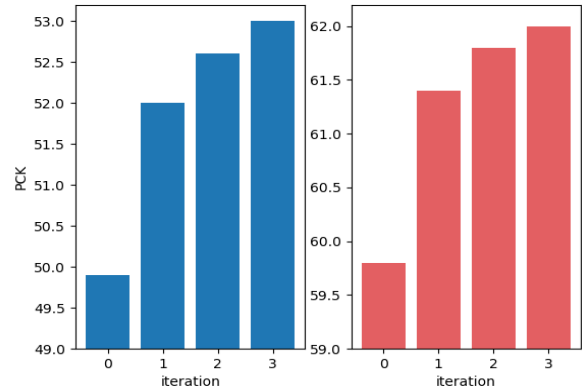


Figure 4: **PCK results at each iteration after iterative training.** We report PCK changes as iterative training repeats and observe the trend of PCK improvements. We use identical architecture for the teacher and student for simplicity, aiming for efficient training as well. We set the iterative training interval to 50 epochs. The left and right figures are the results of MatchMe-CATs and MatchMe-CATs++, respectively.

loss signal, show limited performance improvement compared to the baseline supervised learner (a). This is attributed to their narrow focus on augmenting labels within a limited amount of labeled data. Unlike them, our method (d) focuses on densifying pseudo-labels even with *unlabeled* data as well as labeled data, thereby highly boosting performance.

Analyzing Our Method

Impact of iterative training. To empirically prove the effectiveness of iterative training with the teacher-student framework, Fig. 4 shows the improved PCK values as iterative training progressed. We change the new teacher with the previous student at each iteration and train the student using machine-annotated correspondences, relabeled by the new teacher. As shown in Fig. 4, the performance is consistently improved, and the difference between the first and the last iteration is close to 3% with the same training hyperparameters. This demonstrates that an improved teacher can also improve the student by generating new labels with challenging correspondences that the initial teacher cannot provide.

Robustness evaluation. We verify our method’s robustness by evaluating whether the model can robustly predict correspondences on corrupted images. Since no corrupted or noise-injected datasets exist for dense correspondence learning, we construct a new benchmark for semantic correspondence estimation robustness, named *SPair-C*, following the regime (Hendrycks and Dietterich 2019). Additional details for the dataset are provided in the supplementary material.

Tab. 4 shows the overall PCK values throughout 15 corruptions in SPair-C for MatchMe-CATs versus CATs. We observe that MatchMe-CATs consistently outperforms the baseline (Cho et al. 2021) in terms of the average PCK values across different severities of a single corruption (located in the column of the table) and across different types of corruption with the same severity (shown in the row of the table). Moreover, the average PCK for all 75 corruptions of MatchMe-CATs is 40.9, which represents a 4.2 improvement over the baseline, surpassing the gap of 3.1 observed

Instead of using a sizeable complicated model with strong data augmentations to augment paired images, we have aimed to break the stereotype of using given labeled image pairs by expanding the training pairs with machine-annotated unpaired images. Only with a simple teacher-student framework for labeling the unpaired images, our method could beat the state-of-the-art models on SPair-71k, PF-PASCAL, and PF-WILLOW by large margins. Additionally, our approach could continuously achieve improved performance by repeating the training process iteratively with increasingly challenging image pairs after each step. It also turns out that a resultant model has become more robust to corrupted images.

Limitations. Going beyond the scale of SPair-71k and tackling more challenging datasets unrelated to the semantic correspondence task would reveal a more generalized impact of our work. Furthermore, an exciting direction can be utilizing the recently proposed Transformer-based architecture to deal with the unpaired data with expanded data.

References

Bristow, H.; Valmadre, J.; and Lucey, S. 2015. Dense semantic correspondence where every pixel is a classifier. In *Proceedings of the IEEE International Conference on Computer Vision*, 4024–4031.

Cho, S.; Hong, S.; Jeon, S.; Lee, Y.; Sohn, K.; and Kim, S. 2021. Semantic Correspondence with Transformers. *arXiv preprint arXiv:2106.02520*.

Cho, S.; Hong, S.; and Kim, S. 2022. CATs++: Boosting Cost Aggregation with Convolutions and Transformers. *arXiv preprint arXiv:2202.06817*.

Coates, A.; Ng, A.; and Lee, H. 2011. An analysis of single-layer networks in unsupervised feature learning. In *AISTATS*.

Everingham, M.; Eslami, S. A.; Van Gool, L.; Williams, C. K.; Winn, J.; and Zisserman, A. 2015. The pascal visual object classes challenge: A retrospective. *International journal of computer vision*, 111(1): 98–136.

Ham, B.; Cho, M.; Schmid, C.; and Ponce, J. 2017. Proposal flow: Semantic correspondences from object proposals. *IEEE Transactions on Pattern Analysis and Machine Intelligence*, 40(7): 1711–1725.

Han, K.; Rezende, R. S.; Ham, B.; Wong, K.-Y. K.; Cho, M.; Schmid, C.; and Ponce, J. 2017. Scnet: Learning semantic correspondence. In *Proceedings of the IEEE International Conference on Computer Vision*, 1831–1840.

Hendrycks, D.; and Dietterich, T. 2019. Benchmarking neural network robustness to common corruptions and perturbations. *arXiv preprint arXiv:1903.12261*.

Hosni, A.; Rhemann, C.; Bleyer, M.; Rother, C.; and Gelautz, M. 2012. Fast cost-volume filtering for visual correspondence and beyond. *IEEE Transactions on Pattern Analysis and Machine Intelligence*, 35(2): 504–511.

Huang, S.; Wang, Q.; Zhang, S.; Yan, S.; and He, X. 2019. Dynamic context correspondence network for semantic alignment. In *Proceedings of the IEEE International Conference on Computer Vision*, 2010–2019.

Huang, S.; Yang, L.; He, B.; Zhang, S.; He, X.; and Shrivastava, A. 2022. Learning Semantic Correspondence with Sparse Annotations. In *Computer Vision–ECCV 2022: 17th European Conference, Tel Aviv, Israel, October 23–27, 2022, Proceedings, Part XIV*, 267–284. Springer.

Hui, T.-W.; Tang, X.; and Loy, C. C. 2018. Liteflownet: A lightweight convolutional neural network for optical flow estimation. In *Proceedings of the IEEE Conference on Computer Vision and Pattern Recognition*, 8981–8989.

Hur, J.; Lim, H.; Park, C.; and Chul Ahn, S. 2015. Generalized deformable spatial pyramid: Geometry-preserving dense correspondence estimation. In *Proceedings of the IEEE Conference on Computer Vision and Pattern Recognition*, 1392–1400.

Ilg, E.; Mayer, N.; Saikia, T.; Keuper, M.; Dosovitskiy, A.; and Brox, T. 2017. Flownet 2.0: Evolution of optical flow estimation with deep networks. In *Proceedings of the IEEE conference on computer vision and pattern recognition*, 2462–2470.

Jeon, S.; Min, D.; Kim, S.; Choe, J.; and Sohn, K. 2020. Guided semantic flow. In *European Conference on Computer Vision*, 631–648. Springer.

Kim, J.; Ryoo, K.; Seo, J.; Lee, G.; Kim, D.; Cho, H.; and Kim, S. 2022. Semi-Supervised Learning of Semantic Correspondence with Pseudo-Labels. In *Proceedings of the IEEE/CVF Conference on Computer Vision and Pattern Recognition*, 19699–19709.

Kim, S.; Min, D.; Jeong, S.; Kim, S.; Jeon, S.; and Sohn, K. 2019. Semantic attribute matching networks. In *Proceedings of the IEEE Conference on Computer Vision and Pattern Recognition*, 12339–12348.

Kokkinos, F.; and Kokkinos, I. 2021. Learning monocular 3D reconstruction of articulated categories from motion. In *Proceedings of the IEEE/CVF Conference on Computer Vision and Pattern Recognition*, 1737–1746.

Laskar, Z.; and Kannala, J. 2018. Semi-Supervised Semantic Matching. In *Proceedings of the European Conference on Computer Vision (ECCV) Workshops*, 0–0.

Lee, D.-H.; et al. 2013. Pseudo-label: The simple and efficient semi-supervised learning method for deep neural networks. In *Workshop on challenges in representation learning, ICML*, 896.

Lee, J.; Kim, D.; Ponce, J.; and Ham, B. 2019. Sfnet: Learning object-aware semantic correspondence. In *Proceedings of the IEEE Conference on Computer Vision and Pattern Recognition*, 2278–2287.

Lee, J.; Kim, E.; Lee, Y.; Kim, D.; Chang, J.; and Choo, J. 2020. Reference-based sketch image colorization using augmented-self reference and dense semantic correspondence. In *Proceedings of the IEEE Conference on Computer Vision and Pattern Recognition*, 5801–5810.

Lee, J. Y.; DeGol, J.; Fragoso, V.; and Sinha, S. N. 2021. Patchmatch-based neighborhood consensus for semantic correspondence. In *Proceedings of the IEEE Conference on Computer Vision and Pattern Recognition*, 13153–13163.

Li, H.; Wu, Z.; Shrivastava, A.; and Davis, L. S. 2022. Rethinking pseudo labels for semi-supervised object detection. In *Proceedings of the AAAI Conference on Artificial Intelligence*, 1314–1322.

Li, S.; Han, K.; Costain, T. W.; Howard-Jenkins, H.; and Prisacariu, V. 2020a. Correspondence networks with adaptive neighbourhood consensus. In *Proceedings of the IEEE Conference on Computer Vision and Pattern Recognition*, 10196–10205.

Li, X.; Fan, D.-P.; Yang, F.; Luo, A.; Cheng, H.; and Liu, Z. 2021. Probabilistic Model Distillation for Semantic Correspondence. In *Proceedings of the IEEE Conference on Computer Vision and Pattern Recognition*, 7505–7514.

Li, X.; Liu, S.; De Mello, S.; Kim, K.; Wang, X.; Yang, M.-H.; and Kautz, J. 2020b. Online adaptation for consistent mesh reconstruction in the wild. *Advances in Neural Information Processing Systems*, 33: 15009–15019.

Liu, C.; Yuen, J.; and Torralba, A. 2010. Sift flow: Dense correspondence across scenes and its applications. *IEEE Transactions on Pattern Analysis and Machine Intelligence*, 33(5): 978–994.

Liu, Y.; Zhu, L.; Yamada, M.; and Yang, Y. 2020. Semantic correspondence as an optimal transport problem. In *Proceedings of the IEEE Conference on Computer Vision and Pattern Recognition*, 4463–4472.

Melekhov, I.; Tiulpin, A.; Sattler, T.; Pollefeys, M.; Rahtu, E.; and Kannala, J. 2019. Dgc-net: Dense geometric correspondence network. In *IEEE Winter Conference on Applications of Computer Vision*, 1034–1042. IEEE.

Min, J.; and Cho, M. 2021. Convolutional Hough Matching Networks. In *Proceedings of the IEEE Conference on Computer Vision and Pattern Recognition*, 2940–2950.

Min, J.; Kang, D.; and Cho, M. 2021. Hypercorrelation squeeze for few-shot segmentation. In *Proceedings of the IEEE/CVF International Conference on Computer Vision*, 6941–6952.

Min, J.; Lee, J.; Ponce, J.; and Cho, M. 2019a. Hyperpixel flow: Semantic correspondence with multi-layer neural features. In *Proceedings of the IEEE International Conference on Computer Vision*, 3395–3404.

Min, J.; Lee, J.; Ponce, J.; and Cho, M. 2019b. Spair-71k: A large-scale benchmark for semantic correspondence. *arXiv preprint arXiv:1908.10543*.

Min, J.; Lee, J.; Ponce, J.; and Cho, M. 2020. Learning to compose hypercolumns for visual correspondence. In *Computer Vision–ECCV 2020: 16th European Conference, Glasgow, UK, August 23–28, 2020, Proceedings, Part XV 16*, 346–363. Springer.

Pham, H.; Dai, Z.; Xie, Q.; and Le, Q. V. 2021. Meta pseudo labels. In *Proceedings of the IEEE/CVF Conference on Computer Vision and Pattern Recognition*.

Rasmus, A.; Berglund, M.; Honkala, M.; Valpola, H.; and Raiko, T. 2015. Semi-supervised learning with ladder networks. *Advances in Neural Information Processing Systems*, 28.

Rizve, M. N.; Duarte, K.; Rawat, Y. S.; and Shah, M. 2021. In defense of pseudo-labeling: An uncertainty-aware pseudo-label selection framework for semi-supervised learning. *arXiv:2101.06329*.

Rocco, I.; Arandjelovic, R.; and Sivic, J. 2017. Convolutional neural network architecture for geometric matching. In *Proceedings of the IEEE Conference on Computer Vision and Pattern Recognition*, 6148–6157.

Rocco, I.; Cimpoi, M.; Arandjelovic, R.; Torii, A.; Pajdla, T.; and Sivic, J. 2020. NCNet: Neighbourhood consensus networks for estimating image correspondences. *IEEE Transactions on Pattern Analysis and Machine Intelligence*.

Russakovsky, O.; Deng, J.; Su, H.; Krause, J.; Satheesh, S.; Ma, S.; Huang, Z.; Karpathy, A.; Khosla, A.; Bernstein, M.; et al. 2015. Imagenet large scale visual recognition challenge. *IJCV*.

Sarlin, P.-E.; DeTone, D.; Malisiewicz, T.; and Rabinovich, A. 2020. SuperGlue: Learning feature matching with graph neural networks. In *Proceedings of the IEEE Conference on Computer Vision and Pattern Recognition*, 4938–4947.

Shi, W.; Gong, Y.; Ding, C.; Tao, Z. M.; and Zheng, N. 2018. Transductive semi-supervised deep learning using min-max features. In *Proceedings of the European Conference on Computer Vision*, 299–315.

Sohn, K.; Berthelot, D.; Carlini, N.; Zhang, Z.; Zhang, H.; Raffel, C. A.; Cubuk, E. D.; Kurakin, A.; and Li, C.-L. 2020. Fixmatch: Simplifying semi-supervised learning with consistency and confidence. In *Advances in Neural Information Processing Systems*.

Sun, D.; Yang, X.; Liu, M.-Y.; and Kautz, J. 2018. Pwc-net: Cnn for optical flow using pyramid, warping, and cost volume. In *Proceedings of the IEEE Conference on Computer Vision and Pattern Recognition*, 8934–8943.

Tan, M.; and Le, Q. 2021. Efficientnetv2: Smaller models and faster training. In *International Conference on Machine Learning*, 10096–10106.

Tarvainen, A.; and Valpola, H. 2017. Mean teachers are better role models: Weight-averaged consistency targets improve semi-supervised deep learning results. In *Advances in Neural Information Processing Systems*.

Truong, P.; Danelljan, M.; and Timofte, R. 2020. GLU-Net: Global-local universal network for dense flow and correspondences. In *Proceedings of the IEEE Conference on Computer Vision and Pattern Recognition*, 6258–6268.

Truong, P.; Danelljan, M.; Yu, F.; and Van Gool, L. 2021. Warp Consistency for Unsupervised Learning of Dense Correspondences. In *Proceedings of the IEEE International Conference on Computer Vision*, 10346–10356.

Truong, P.; Danelljan, M.; Yu, F.; and Van Gool, L. 2022. Probabilistic Warp Consistency for Weakly-Supervised Semantic Correspondences. *arXiv preprint arXiv:2203.04279*.

Xie, G.-S.; Xiong, H.; Liu, J.; Yao, Y.; and Shao, L. 2021. Few-shot semantic segmentation with cyclic memory network. In *Proceedings of the IEEE/CVF International Conference on Computer Vision*, 7293–7302.

Xie, Q.; Dai, Z.; Hovy, E.; Luong, T.; and Le, Q. 2020a. Unsupervised data augmentation for consistency training. In *Advances in Neural Information Processing Systems*.

Xie, Q.; Luong, M.-T.; Hovy, E.; and Le, Q. V. 2020b. Self-training with noisy student improves imagenet classification. In *Proceedings of the IEEE/CVF Conference on Computer Vision and Pattern Recognition*.

Xu, Y.; Shang, L.; Ye, J.; Qian, Q.; Li, Y.-F.; Sun, B.; Li, H.; and Jin, R. 2021. Dash: Semi-supervised learning with dynamic thresholding. In *International Conference on Machine Learning*.

Yang, G.; and Ramanan, D. 2019. Volumetric correspondence networks for optical flow. *Advances in Neural Information Processing Systems*, 32.

Yun, S.; Oh, S. J.; Heo, B.; Han, D.; Choe, J.; and Chun, S. 2021. Re-labeling imagenet: from single to multi-labels, from global to localized labels. In *Proceedings of the IEEE/CVF Conference on Computer Vision and Pattern Recognition*, 2340–2350.

Zhang, B.; Wang, Y.; Hou, W.; Wu, H.; Wang, J.; Okumura, M.; and Shinohzaki, T. 2021. Flexmatch: Boosting semi-supervised learning with curriculum pseudo labeling. In *Advances in Neural Information Processing Systems*.

Zhao, D.; Song, Z.; Ji, Z.; Zhao, G.; Ge, W.; and Yu, Y. 2021. Multi-scale Matching Networks for Semantic Correspondence. In *Proceedings of the IEEE International Conference on Computer Vision*, 3354–3364.

Appendix

In this document, we include additional details that include various aspects of our research as follows:

- **Robustness Evaluation Benchmark:** We introduce a new robustness benchmark for semantic correspondence, named **SPair-C**, providing comprehensive descriptions of its details.
- **Further Analysis:** We present an ablation study and analysis to understand the performance of our method further.
- **Visualizations:** We showcase qualitative results by comparing our method with state-of-the-art methods.
- **Further Details of Training:** We provide additional detail of our method, emphasizing how we utilize unlabeled data to enhance performance.

Robustness Evaluation Benchmark

We introduce a new corruption benchmark to verify the robustness of dense correspondence learning methods. This benchmark, which is the corrupted SPair, is dubbed SPair-C, as mentioned in the Robustness evaluation section of the main paper. Its purpose is to complement the existing dense correspondence learning task by providing a more challenging dataset for evaluating the robustness of models.

Dataset Details

Since hardly corrupted or noise-injected images have been used to evaluate dense correspondence learning, we construct a new corruption robustness benchmark for semantic correspondence following the existing regime (Hendrycks and Dietterich 2019). The future applicability of a model can be measured by evaluating the robustness of corrupted images involving frequently observed corruptions occurring in the wild.

Fig. A shows 15 types of corruptions in the SPair-C dataset, selected among corruptions (Hendrycks and Dietterich 2019) used for measuring robustness. We choose appropriate corruptions for pixel-level prediction from noise, blurred weather, and digital categories, which do not affect significant point changes after corruptions. The finalized categories are noise (Gaussian, shot, impulse, and speckle), blur (defocus and Gaussian), weather (snow, frost, fog, and spatter), and digital categories (brightness, contrast, saturate, pixelated, and JPEG); we apply the five levels of the severity s per each type of corruption exemplified in Fig. B. Therefore, a set of 75 common visual corruptions, which enable models to be fooled by small changes in the original image, are used for one test image. We use the codebase¹ to build the benchmark.

Further Analysis

In this section, we first ablate our model regarding the confidence threshold. Then, we analyze PCK concerning the tolerance threshold α . Finally, we qualitatively compare our method with the competing methods.

¹<https://github.com/hendrycks/robustness>

Confidence threshold (τ)	PCK
0.1	52.7
0.3	52.6
0.5	52.6
0.7	53.0
0.9	52.3

Table A: **Impact of machine-annotated data.** We study the sensitivity of PCK as the quantity and quality of machine-annotated data change by the confidence threshold τ . We adjust τ from 0.1 to 0.9 and confirm how PCK changes. CATs (Cho et al. 2021) is used for this study. We observe the model can yield the maximal PCK with the tuned τ but shows insensitive PCKs to τ .

Ablation on Confidence Threshold

The confidence threshold τ in Eq.(8) is a critical hyper-parameter that determines the quantity and quality of machine-annotated data used for training. To investigate the relationship between the confidence threshold and model performance, we conduct an ablation study with the threshold at intervals of 0.2 across a wide range of confidence thresholds from 0.1 to 0.9. We use CATs (Cho et al. 2021) for this study.

As shown in Tab. A, while the threshold value of 0.7 produces the highest PCK value, other values do not significantly degrade performance and still have higher PCK values than the baseline's PCK 49.9, which do not use our method. Increasing the amount of pseudo-labeled data by lowering the threshold (e.g., $\tau \leq 0.3$) results in better performance than improving the quality of pseudo-labeled data by raising the confidence threshold (e.g., $\tau = 0.9$). However, the overall trend demonstrates that the model is not sensitive to adjusting the threshold and that the use of machine-annotated data is an essential factor in model performance.

PCK Analysis

The main paper presents Tab. 1, which shows a significant performance improvement at PCK@0.1 compared with previous state-of-the-art methods. We report PCK results with the various tolerance thresholds from 0.1 to 0.01 on SPair-71k in comparison between ours and SOTA baselines (Coates, Ng, and Lee 2011; Cho, Hong, and Kim 2022; Kim et al. 2022; Huang et al. 2022) in Tab. B. The results demonstrate that our expanded pseudo-labeled point correspondences amplified at pixel-level and image-level can make the trained model more accurately estimate the correspondences, as evidenced by the significant PCK gaps with much stricter tolerance criteria, with smaller α values, compared to other methods. Moreover, the results show that as the tolerance threshold of PCK (α) decreases, the gap with the baseline (Cho, Hong, and Kim 2022) does not narrow but widens. For example, at $\alpha = 0.1$, the performance gap is 2.2, but at $\alpha = 0.05$, it is 4.3, showing a gap of about twice as much. Therefore, this demonstrates that our predicted point correspondences are almost approximate to the GT point correspondences.

Besides analyzing PCK values to quantify model performance, we demonstrate the superiority of our method by visualizing its predictive quality in Fig. C and Fig. D. We compare the difference between the correctly predicted and

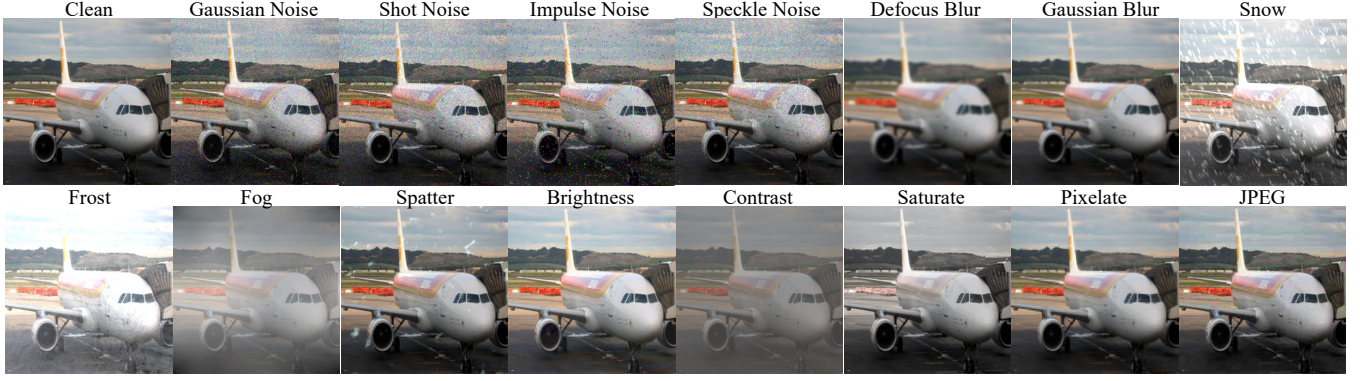


Figure A: **Visualization of corrupted images in SPair-C.** The corrupted images of one sample consist of types of algorithmically generated corruptions from noise, blur, weather, and digital categories. Each type of corruption has five levels of severity, resulting in 75 distinct corruptions.



Figure B: **Corrupted images with different severities.** We visualize a chosen image from SPair-71k (Min et al. 2019b) with severity from 1 to 5. The images get noisier as the severity increases.

the ground truth (GT) point correspondences at $\alpha = 0.1$, as indicated by yellow and green colors, respectively. This visualization illustrates how many more points our model predicts correctly as well as how closely our model's predictions align with the correct GT key points, even at the extreme points compared to the baseline (Cho, Hong, and Kim 2022). Specifically, the example of the sheep class, having the smallest categorical PCK difference compared to the baseline, illustrates that, even though the PCK achieved by our method is similar to that of the baseline, the quality of the predicted correspondence is superior. This outstanding performance can be attributed to the fact that our method generates machine-annotated point correspondences, providing diverse and rare supervisions that are difficult to obtain through the limited amount of manually annotated GT key points.

Visualizations

Comparison with State-of-the-arts

In addition to the qualitative results presented in Fig. 3 of the main paper, we provide further visualizations of example pairs with their predicted matches for MatchMe-CATs++ and the top-performing competing methods in both the supervised and semi-supervised regimes:CATs (Cho et al. 2021), CATs++ (Cho, Hong, and Kim 2022), SemiMatch (Kim et al. 2022), SCORRSAN (Huang et al. 2022). As shown in Fig. E, our approach excels in producing more accurate estimations of correspondences between image pairs across various object classes and differences in variation factors compared

with other methods.

Comparison with semi-supervised methods

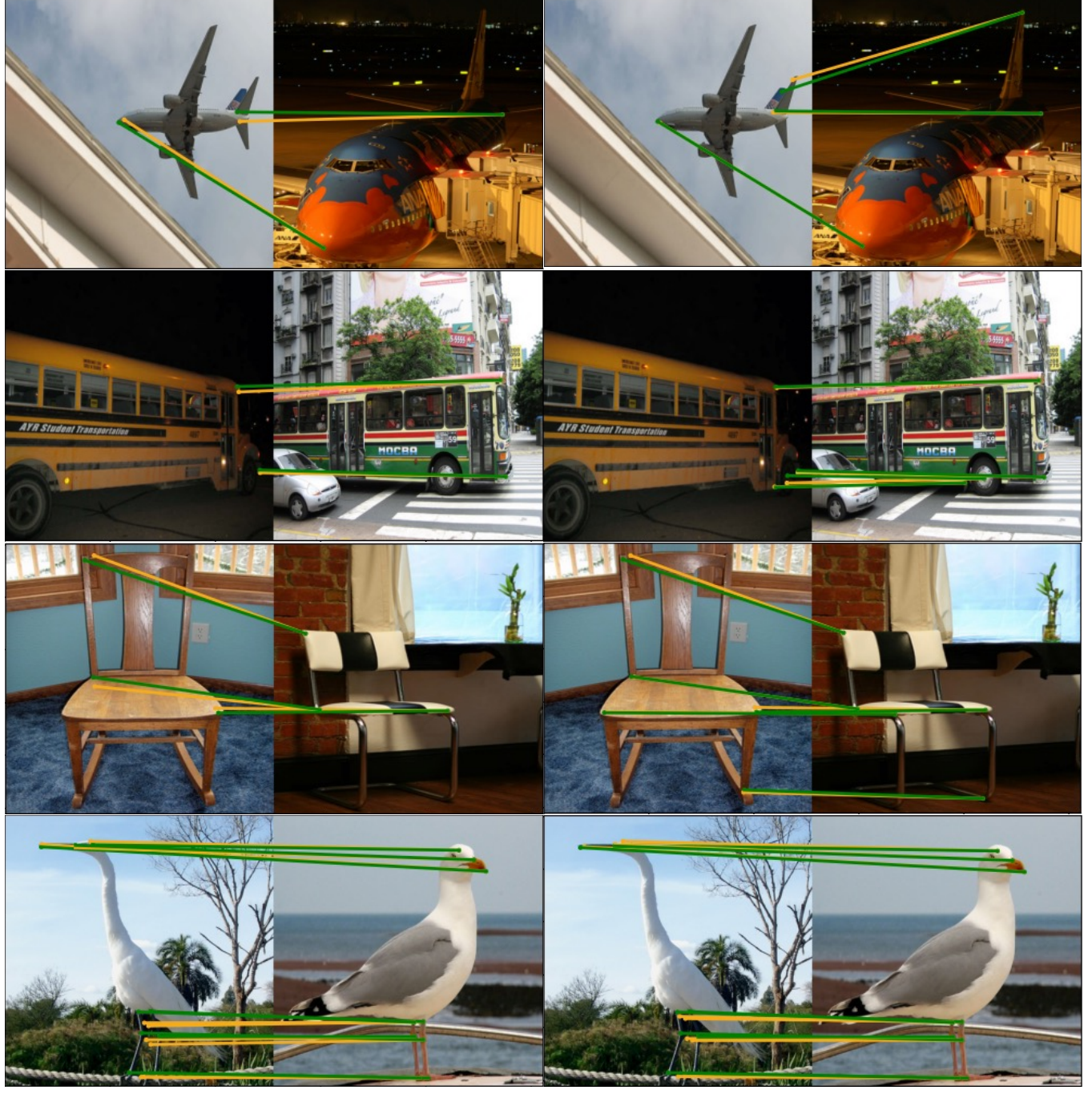
We show qualitative results to complement the controlled experiments in the main paper, where all the methods are trained under the same network architecture, suggested in CATs++ (Cho, Hong, and Kim 2022) for a fair comparison. As shown in Fig. F, we predict correct correspondences, even in challenging samples that exhibit significant differences in scale and viewpoint between image pairs, unlike other methods, which tend to produce incorrect predictions for such samples.

Further Details of Training

We use the labeled data in the training set of SPair-71k (Min et al. 2019b) along with the unlabeled data in PASCAL VOC 2012 (Everingham et al. 2015), which is the source of SPair-71k. We assign images for each object class according to the corresponding classification labels. Only non-overlapping images in the validation and test set of SPair-71k are used for training to avoid cheating. Furthermore, images in the 'dining table' and 'sofa' classes are not included in the same way that the dining table and sofa categories are not used as in SPair-71k. Since SPair-71k has similar numbers of labeled data for each class, we balance the number of unlabeled data for each class to ensure that their distribution matches that of the labeled data. We use different batches of unlabeled data in every iteration to diversify the training sample.

α	0.01	0.02	0.03	0.04	0.05	0.06	0.07	0.08	0.09	0.1
CATs (Cho et al. 2021)	1.93	7.0	13.8	20.9	27.7	33.6	38.6	43.0	46.8	49.9
CATs++ (Cho et al. 2021)	4.3	14.6	25.0	33.9	40.8	46.4	50.8	54.3	57.3	59.8
SemiMatch (Kim et al. 2022)	2.1	7.7	15.0	22.4	29.0	34.8	39.7	43.9	47.6	50.7
SCORRSAN (Huang et al. 2022)	3.6	12.1	21.3	29.3	35.8	41.0	45.2	48.8	51.7	55.3
MatchMe-CATs	2.0	7.2	14.6	22.4	29.6	35.7	41.1	45.7	49.6	53.0
MatchMe-CATs++	6.1	18.5	29.9	38.6	45.1	50.0	53.9	57.0	59.7	62.0

Table B: **PCK comparison with state-the-art methods under varying tolerance (α)**. We report PCK for different α of the state-of-the-art methods on SPair-71k (Min et al. 2019b). Numbers in bold denote the best. MatchMe-CATs++ outperforms all the methods by a large margin.



(a) CATs++

(b) MatchMe-CATs++

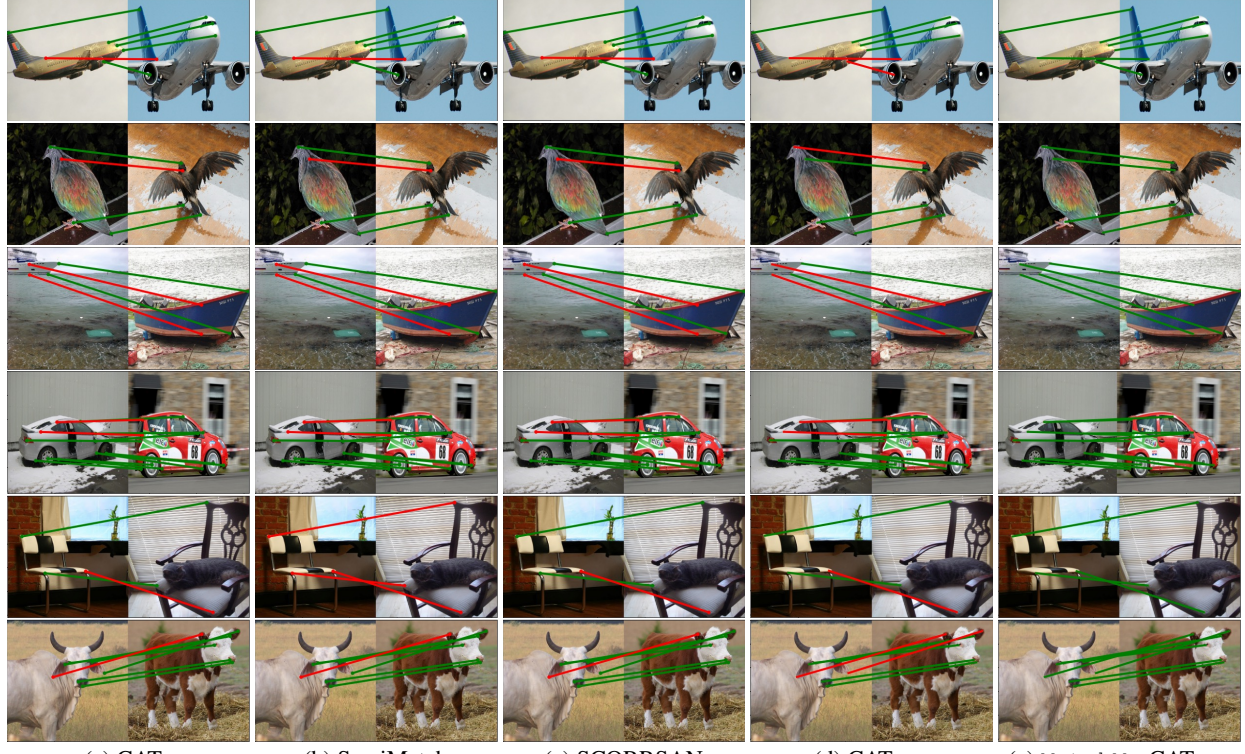
Figure C: **Visualization of the difference between correctly predicted points and ground truth (GT) points on SPair-71k (Min et al. 2019b)**. The GT points in the left image corresponding to the GT points in the right image for each image pair are marked in green lines, and the predicted point correspondences are marked in yellow lines. The closer the predicted correspondence to the GT correspondence is, the more accurate the prediction. Notice that if only the green line is visible, the predicted and GT point correspondences are perfectly matched.



(a) CATs++ (Cho, Hong, and Kim 2022)

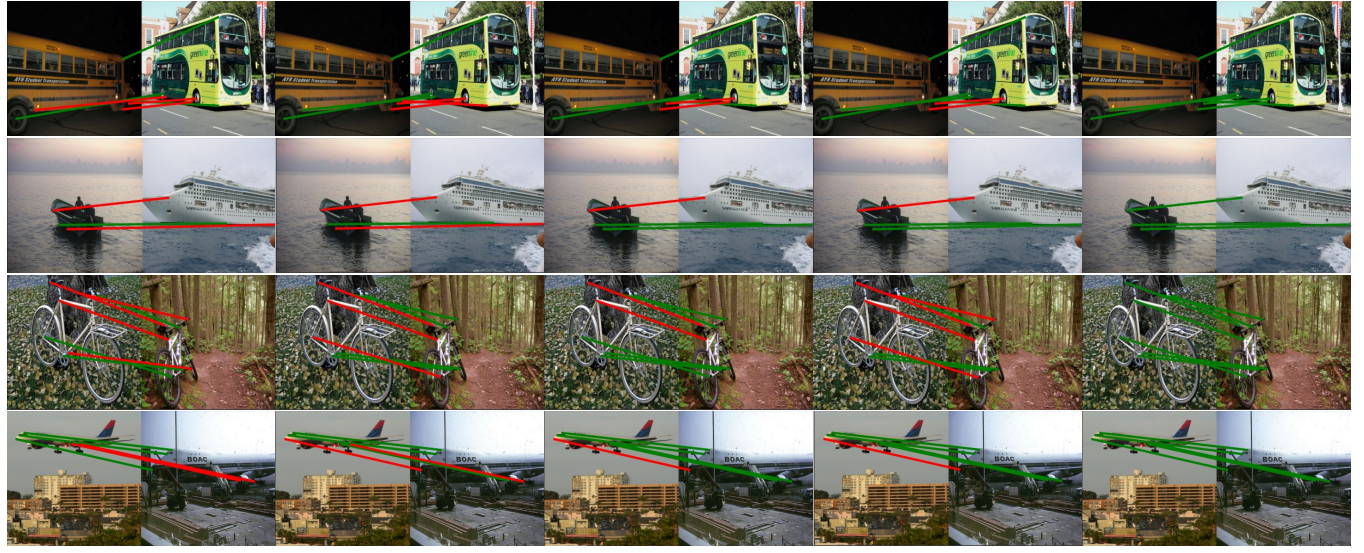
(b) MatchMe-CATs++

Figure D: Visualization of the difference between correctly predicted points and ground truth (GT) points on SPair-71k (Min et al. 2019b) (cont'd). The GT points in the left image corresponding to the GT points in the right image for each image pair are marked in green lines, and the predicted point correspondences are marked in yellow lines. The closer the predicted correspondence to the GT correspondence is, the more accurate the prediction. Notice that if only the green line is visible, the predicted and GT point correspondences are perfectly matched.



(a) CATs (b) SemiMatch (c) SCORRSAN (d) CATs++ (e) MatchMe-CATs++

Figure E: **Qualitative results on SPair-71k in comparison with SOTA methods (cont'd)** The point-to-point matches are drawn by linking key point pairs with line segments. Green and red lines denote correct and incorrect predictions with respect to the ground-truth pairs, respectively. We observe that ours perform much well compared with the counterparts across all the sample image pairs.



(a) CATs++ (b) (a) + CNNGeoU (c) (a) + PWarpC (d) (a) + SCORRSAN (e) (a) + MatchMe

Figure F: **Qualitative results on SPair-71k (Min et al. 2019b) in comparison with other semi-supervised methods:** For a fair comparison, we use the fixed baseline CATs++ (Cho, Hong, and Kim 2022) (a) for all semi-supervised methods, CNNGeoU (Laskar and Kannala 2018) (b), PWarpC (Truong et al. 2022) (c), SCORRSAN (Huang et al. 2022) (d), and MatchMe(d). The point-to-point matches are drawn by linking key point pairs with line segments. Green and red lines denote correct and incorrect predictions with respect to the ground-truth pairs, respectively. We observe that ours perform much well compared with the counterparts across all the sample image pairs.